

Ram pressure stripping of disc galaxies orbiting in clusters. I. Mass and radius of the remaining gas disc

Elke Roediger* and Marcus Brüggen*

Jacobs University Bremen, P.O. Box 750 561, 28725 Bremen, Germany

Accepted. Received; in original form

ABSTRACT

We present the first 3D hydrodynamical simulations of ram pressure stripping of a disc galaxy orbiting in a galaxy cluster. Along the orbit, the ram pressure that this galaxy experiences varies with time. In this paper, we focus on the evolution of the radius and mass of the remaining gas disc and compare it with the classical analytical estimate proposed by Gunn & Gott (1972). We find that this simple estimate works well in predicting the evolution of the radius of the remaining gas disc. Only if the ram pressure increases faster than the stripping timescale, the disc radius remains larger than predicted. However, orbits with such short ram pressure peaks are unlikely to occur in other than compact clusters. Unlike the radius evolution, the mass loss history for the galaxy is not accurately described by the analytical estimate. Generally, in the simulations the galaxy loses its gas more slowly than predicted.

Key words: galaxies: spiral – galaxies: evolution – galaxies: clusters – intergalactic medium

1 INTRODUCTION

Galaxies populate different environments, ranging from isolated field regions to dense galaxy clusters. Depending on the environment, the properties of galaxies, especially disc galaxies, change: In denser regions, disc galaxies tend to contain less neutral gas, show a weaker star formation activity and redder colours than galaxies in sparse regions (e.g. van Gorkom 2004; Goto et al. 2003 and references therein).

Ram pressure stripping (RPS), i.e. the removal of a galaxy’s gas disc due to its motion through the intracluster medium (ICM), is one of the likely candidates to explain these features. Gunn & Gott (1972) (GG72) proposed that for galaxies moving face-on through the ICM the success or failure of RPS can be predicted by comparing the ram pressure with the galactic gravitational restoring force per unit area. Hydrodynamical simulations of RPS presented so far (Abadi et al. 1999, Quilis et al. 2000, Schulz & Struck 2001 (SS01), Marcolini et al. 2003 (MBD03), Roediger & Hensler 2005 (RH05), Roediger & Brüggen 2006 (RB06)) suggest that this analytical estimate does indeed do a fair job as long as the galaxies are not moving close to edge-on. However, in all these simulations the model galaxy was not exposed to a varying ICM wind, as one expects for cluster galaxies, but to a constant one. A few 2D simulations of spherical galaxies

on radial orbits in clusters (Lea & Young 1976, Takeda et al. 1984, Acreman et al. 2003) exist, where the early ones were run with low resolution. Toniazzo & Schindler (2001) presented 3D hydro-simulations for a spherical galaxy on a cluster orbit. Vollmer et al. (e.g. 1999, 2000, 2001, 2001a, 2003) have simulated the cluster passage of disc galaxies with a sticky-particle code, where the ram pressure is modelled as an additional force on the disc gas particles. Their work shows the importance of the modelling of realistic orbits, e.g. to determine the stripping history of individual galaxies. However, the sticky-particle code cannot model hydrodynamical effects such as instabilities that have been shown to play a role by the hydro-simulations. Additionally, the work of SS01, RH05 and RB06 has shown that the gas removal from the galactic potential does not occur instantaneously, but that it takes some time until the gas is accelerated enough to become unbound from the galaxy’s potential. Thus, in cases of short ram pressure peaks, this time delay may play an important role.

Here we present the first 3D hydrodynamical simulations of RPS of a disc galaxy orbiting in a galaxy cluster. We focus on the question, in how far a time-dependent version of the analytical estimate based on the GG72 criterion can describe the evolution of the remaining gas disc.

* E-mail: e.roediger@jacobs-university.de, m.brueggen@jacobs-university.de

2 METHOD

We model the flight of a disc galaxy through a galaxy cluster. The galaxy starts at a position ~ 1 to 2 Mpc (depending on orbit) from the cluster centre with a given initial velocity. We use analytical potentials for the galaxy and the cluster, as this reduces computational costs significantly. Given the high velocities of cluster galaxies, the tidal effect on the galaxy is expected to be small. The work of Moore et al. (1996, 1998, 1999) demonstrated that only harassment, i.e. the cumulative effect of frequent close high velocity encounters between cluster galaxies and the overall tidal field of the cluster affects cluster galaxies seriously. Thus, we expect that our treatment yields reasonable results.

The orbit of the galaxy is determined by integrating the motion of a point mass through the gravitational potential of the cluster. In the course of the simulation, the position of the galaxy potential is shifted along this orbit.

2.1 Code

The simulations were performed with the FLASH code (Fryxell et al. 2000), a multidimensional adaptive mesh refinement hydrodynamics code. It solves the Riemann problem on a Cartesian grid using the Piecewise-Parabolic Method (PPM). The simulations presented here are performed in 3D. The gas obeys a polytropic equation of state with an adiabatic index of $\gamma = 5/3$. The size of the simulation box is chosen such that the galaxy’s orbit during the simulation time (3 Gyr) fits into the grid. Depending on the orbit, the size of the simulation box ranges between $(2 \text{ Mpc})^3$ and $2 \times 5 \times 2 \text{ Mpc}^3$. For an example see Fig. 1. All boundaries are reflecting.

The coarsest refinement level has a resolution of $\Delta x = 62.5 \text{ kpc}$. For most runs, we use 8 levels of refinement, i.e. the best resolution is $\Delta x = 0.5 \text{ kpc}$. In addition to the standard density and pressure gradient criteria, our user-defined refinement criteria enforce maximal refinement on the galactic gas disc and enforce stepwise de-refinement with increasing distance to the galaxy in the following fashion:

- We always refine a sphere of radius 50 kpc around the galaxy centre to at least $\Delta x = 3.9 \text{ kpc}$ (5 refinement levels).
- We always use the maximum refinement level for the galactic disc region, which is defined as the cylinder with radius 27 kpc and thickness 6 kpc around galactic centre, where the density larger than $10^{-27} \text{ g cm}^{-3}$.
- We limit the refinement outside 50 kpc around galaxy centre to $\Delta x = 2 \text{ kpc}$ (6 refinement levels).
- We limit the refinement outside 150 kpc around galaxy centre to $\Delta x = 15.6 \text{ kpc}$ (3 refinement levels).
- Additionally, we always refine a sphere of radius 100 kpc around cluster centre to $\Delta x = 7.8 \text{ kpc}$ (4 refinement levels).

Our user-defined de-refinement rules overwrite the standard pressure and density gradient criteria, but our user-defined refinement criteria overwrite the de-refinement criteria. The FLASH code also ensures that neighbouring blocks differ by maximal one refinement level.

A detailed discussion of the influence of the resolution on our results is given in Sect. A.

2.2 Model galaxy

The galaxy model is the same as in RB06, i.e. a massive spiral with a flat rotation curve at 200 km s^{-1} . It consists of a dark matter halo, a stellar bulge, a stellar disc and a gaseous disc. All non-gaseous components just provide the galaxy’s potential and are not evolved during the simulation. For a description of the individual components and a list of parameters please refer to RB06.

Initially, the galaxy is set in pressure equilibrium with the surrounding ICM. For the case of a homogeneous ICM density and pressure, this task is straightforward. In our case, however, there is the difficulty that both, pressure and density of surrounding ICM, vary with distance from the cluster centre. Consequently, the ICM pressure at the ”surface” of the galaxy is not the same everywhere. Therefore, we use the following procedure for setting the galaxy in pressure equilibrium with the surrounding ICM:

(i) We chose values for the ICM density and pressure somewhat lower than the values at the galaxy’s initial position.

(ii) We calculate the density, pressure and rotation velocity in the galaxy’s gas disc such that the gas disc is in pressure equilibrium with a homogeneous ambient gas of density and pressure chosen in (i).

(iii) We now need to ensure a continuous transition from the galactic disc to the cluster ICM. Therefore, we compare the pressure calculated in (ii) with the ICM pressure in each grid cell. Inside the gas disc the pressure calculated in (ii) is larger than the ICM pressure. However, at the transition to the ambient gas used in (ii), the pressure set in (ii) will be lower than the ICM pressure. In such grid cells, we substitute the values from (ii) with ICM values. This ensures that the pressure distribution is continuous everywhere. However, the density distribution shows a jump between the ICM and the ISM. Rotation velocity plus initial orbital velocity is only set for ISM cells.

Figure 2 displays radial profiles for the density, projected ISM surface density, pressure, and total velocity in the galactic plane for two runs. The galaxy’s initial position in these two runs differs (see Table 2). Therefore, the gas discs have to be in pressure equilibrium with different external pressures and thus differ slightly in radius. Moreover, the radius of each gas disc varies slightly with azimuthal angle, because the pressure in the ICM surrounding the galaxy is not homogeneous. However, at least in the inner 10 kpc, the profiles of different runs are indistinguishable.

2.3 Cluster model

The cluster is set in hydrostatic equilibrium, where the density of the ICM follows a β -profile,

$$\rho_{\text{ICM}}(r) = \rho_{\text{ICM}0} \left[1 + \left(\frac{r}{R_{\text{ICM}}} \right)^2 \right]^{-3/2\beta}, \quad (1)$$

while the ICM temperature is constant. Here we present simulations for three clusters. The parameters are listed in Table 1. Figure 3 shows the density and pressure profiles of clusters C1 and C3. The only difference between clusters C1 and C2 is a factor of 2 in the density. These two clusters are compact, the ICM density is strongly peaked. Thus, they

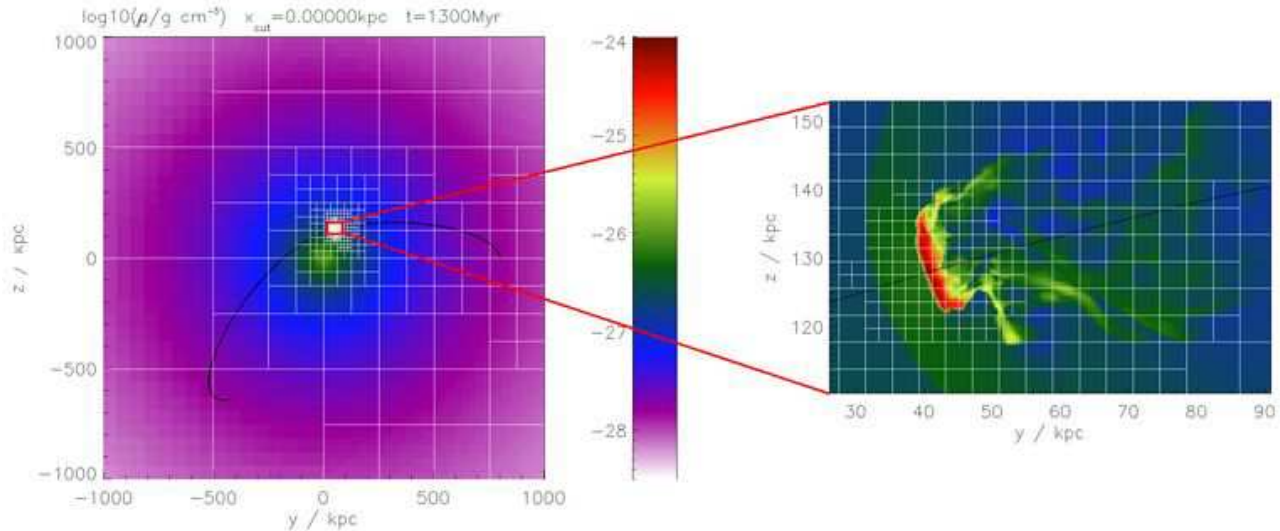


Figure 1. Colour-coded gas density in the orbital plane for run C2-SM-SLW-MFM (here with best resolution 0.25 kpc). The lhs picture shows a slice through the complete simulation box, the rhs a blow-up of the region around the galaxy. The black line marks the galaxy’s orbit. The white rectangles show the adaptive grid: Each rectangle marks the boundaries of one block, each block consists of 8^3 grid cells.

Table 1. ICM parameters: Core radius, R_{ICM} , beta-parameter, β , central ICM density, $\rho_{\text{ICM}0}$, and ICM temperature, T_{ICM} , for clusters C1, C2 and C3.

	$R_{\text{ICM}}/\text{kpc}$	β	$\rho_{\text{ICM}0}/(\text{g cm}^{-3})$	T_{ICM}/K
C1	50	0.5	$2 \cdot 10^{-26}$	$4.7 \cdot 10^7$
C2	.	.	10^{-26}	.
C3	386	0.705	$6.07 \cdot 10^{-27}$	$9.5 \cdot 10^7$

are similar to the Virgo cluster (Matsumoto et al. 2000), but not as extreme as Virgo (see Fig. 3). Cluster C3 resembles the Coma cluster (parameters see Mohr et al. 1999), which is very extended.

2.4 Galaxy orbit

The orbit of the galaxy determines its ram pressure history. According to the simulations of RB06, for our model galaxy, complete stripping is expected for ram pressures of about $10^{-10} \text{ erg cm}^{-3}$. We will refer to such ram pressures as “high”. “Medium” ram pressures ($\sim 10^{-11} \text{ erg cm}^{-3}$) are still expected to strip the gas disc significantly. We aimed at constructing orbits with medium to high ram pressure peaks. Moreover, we concentrate on orbits of galaxies that could be regarded as falling into the cluster for the first time, i.e. they start from a sufficiently large distance from the cluster centre. Additionally, the galaxies are bound to the cluster.

Figure 4 shows several representative orbits in clusters C1 and C3. Already at this stage some important issues can be learned:

- Naturally, orbits with large impact parameters yield ram pressure peaks of long duration. Short ram pressure peaks are typical for galaxies passing near the cluster centre. However, even on orbits with small impact parameters,

the ram pressure peaks in the extended cluster are about twice as wide as on comparable orbits in the compact cluster.

- Orbits with low ram pressure peaks are practically impossible in both, the extended and the compact cluster. Even on orbits with large impact parameter, where the ICM density along the orbit is small, the galaxy’s velocity is high enough to yield at least medium ram pressures. If the galaxy passes near the cluster centre, typically both, ICM density and galaxy velocity are high.

- In the extended cluster, even orbits with medium ram pressure peaks are difficult to construct. Almost all galaxies should be stripped severely or completely.

- Comparing the pressure profile along the galactic disc as shown in Fig. 2 with the radial pressure profiles of the clusters (Fig. 3) gives an interesting insight into the importance of the cluster environment for the galaxy: The ICM-pressure in the Coma-like cluster drops below $10^{-12} \text{ erg cm}^{-3}$ only for radii larger than $\sim 2 \text{ Mpc}$. Inside $\sim 1 \text{ Mpc}$ the ICM pressure is above $10^{-11} \text{ erg cm}^{-3}$. These values are comparable to the pressure in the galactic plane at disc radii of approx. 15 and 8 kpc. Thus, even if a galaxy could reach such a position in the cluster without suffering from any other processes, its gas disc should be affected at least by the external pressure.

- During most of the orbit, the ram pressure is even larger than the thermal ICM pressure (bottom panel of Fig. 5).

Here we present simulations for four orbits that are summarised in Fig. 5. The labels of the runs represent the cluster (C+number), small or large impact parameter (SM or LG), fast or slow galaxy (FST or SLW), inclination (F for near face-on, M for medium, E for near edge-on; FE for first near face-on but then near edge-on, etc.). In all cases, the galaxy orbits in the y - z -plane. Table 2 lists the simulation runs.

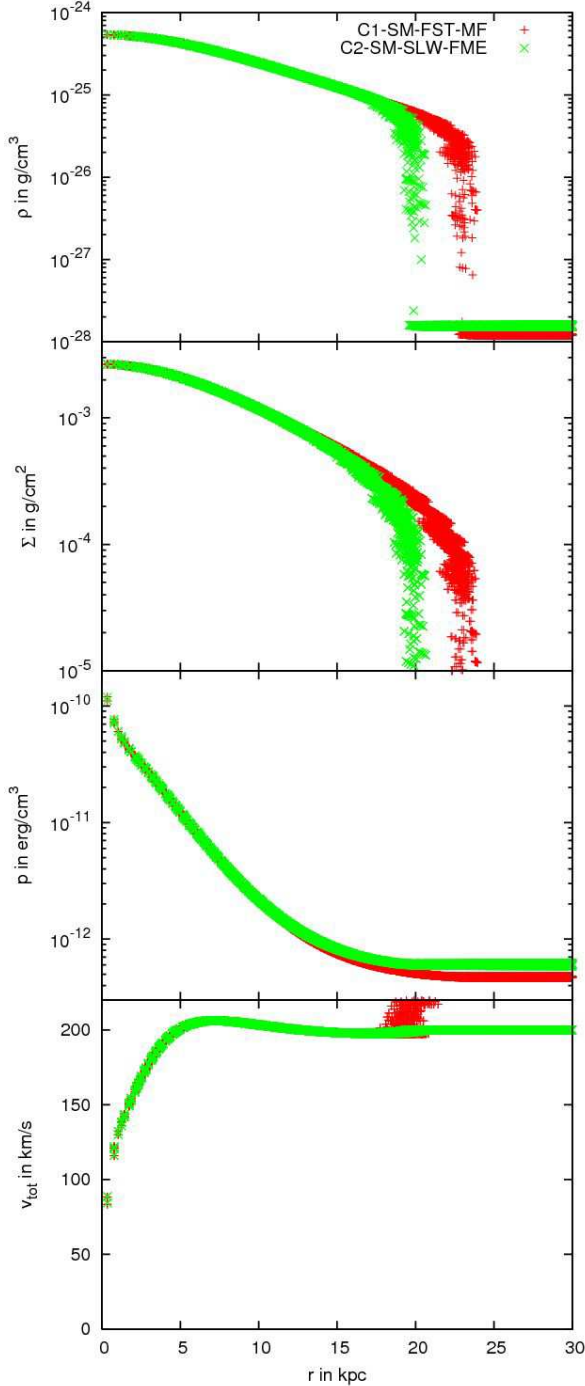


Figure 2. Radial profiles of the density, ρ , pressure, p , and total velocity, v_{tot} , in the galactic plane for the initial model for two different runs (see legend). Also the radial profile for the projected ISM surface density, Σ , is shown. One dot for each cell in the galactic plane is plotted. In the bottom panel, the total velocity in the galaxy’s rest frame is shown. Velocities inside the disc radius (as set by e.g. the density profile) are due to the galaxy’s rotation, while velocities outside the disc radius are due to the galaxy’s motion through the ICM.

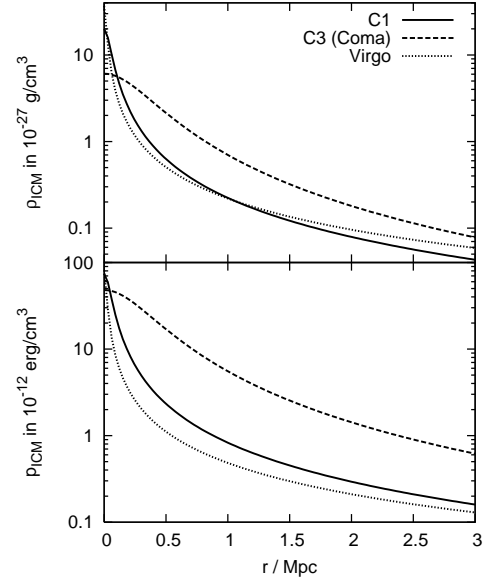


Figure 3. Density and pressure profiles for model clusters C1 and C3. The profiles for cluster C2 are a factor of 2 lower than the ones of cluster C1. For comparison, the profiles for the Virgo cluster are shown.

Table 2. List of runs. Run labels code the cluster (C+number), small or large impact parameter (SM or LG), fast or slow galaxy (FST or SLW), inclination (F for near face-on, M for medium, E for near edge-on; FE for first near face-on but then near edge-on, etc.). Initial galaxy coordinates $x_{\text{gal}0}$ and $z_{\text{gal}0}$ are always zero, $y_{\text{gal}0}$ is given in the second column. The third column lists the initial galaxy velocity. The inclination listed in the fourth column is the angle between the galaxy’s rotation axis and the y -axis.

label	$y_{\text{gal}0}$ in kpc	initial velocity in km s^{-1}	inclination in $^\circ$
C1-SM-FST-MF	1500	(0, -600, 100)	-30
C1-SM-FST-E	.	.	80
C1-LG-FST-MF	1300	(0, -600, 500)	-30
C1-LG-FST-EF	.	.	-60
C1-LG-FST-FE	.	.	45
C2-SM-SLW-FME	800	(0, 0, 200)	30
C2-SM-SLW-EMF	.	.	-60
C2-SM-SLW-MFM	.	.	-20
C3-SM-FST-MF	2300	(0, -800, 200)	30

3 RESULTS

Previous simulations where the galaxy was exposed to a constant ICM wind found that the ICM-ISM interaction is a multi-stage process (SS01, MBD03, RH05, RB06). The stages reflect the two gas removal mechanisms that work on different timescales.

One process is ram pressure “pushing”, the immediate consequence of the ram pressure dislocating the gas disc at radii where the galaxy’s gravity is not strong enough. This process results in the instantaneous stripping phase where the gas is pushed out of its original position on a timescale of a few 10 Myr. However, the gas does not become unbound

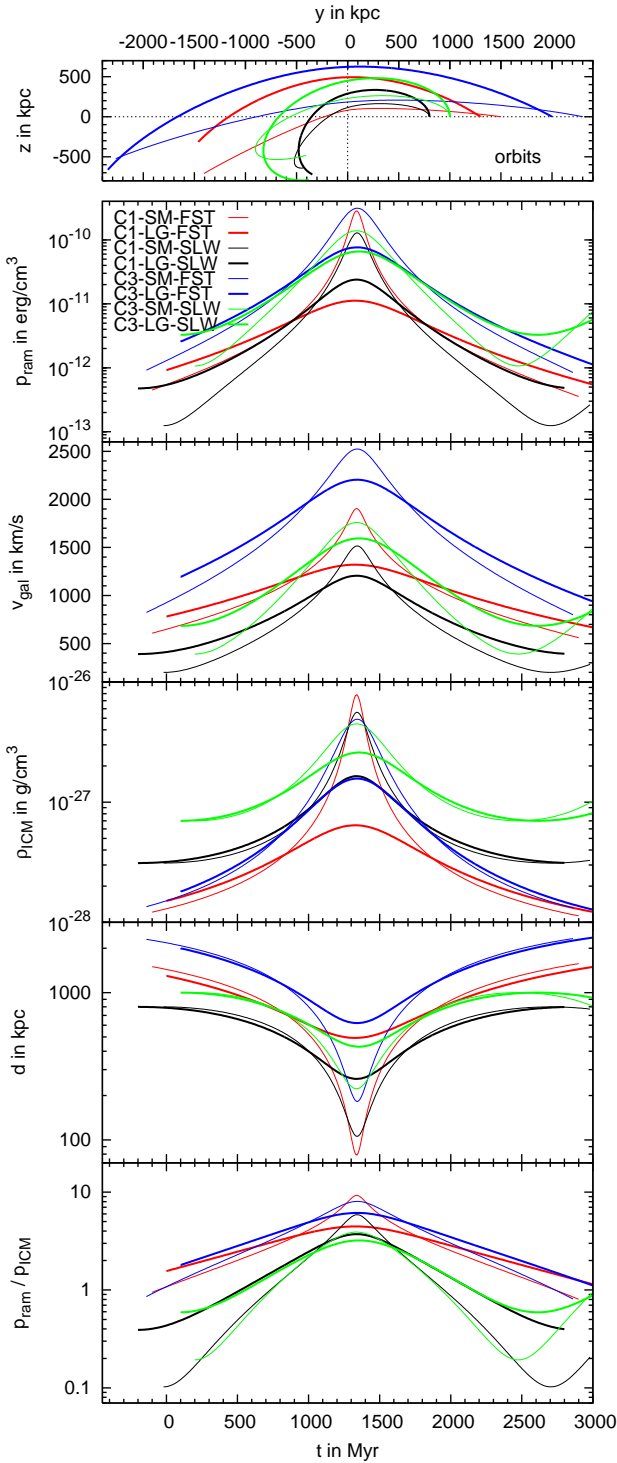


Figure 4. Representative galaxy orbits in clusters C1 and C3: The top panel shows the orbits, which are in the y - z -plane. The next panels show the temporal evolution of ram pressure, p_{ram} , galaxy velocity, v_{gal} , ICM density along orbit, ρ_{ICM} , distance to cluster centre, d , and ratio between ram pressure and local ICM pressure, $p_{\text{ram}}/\rho_{\text{ICM}}$. The clusters (C1 or C3), typical galaxy velocity (FaST or SLoW) and impact parameter (SMall or LarGe) are coded by line colour and thickness, see legend.

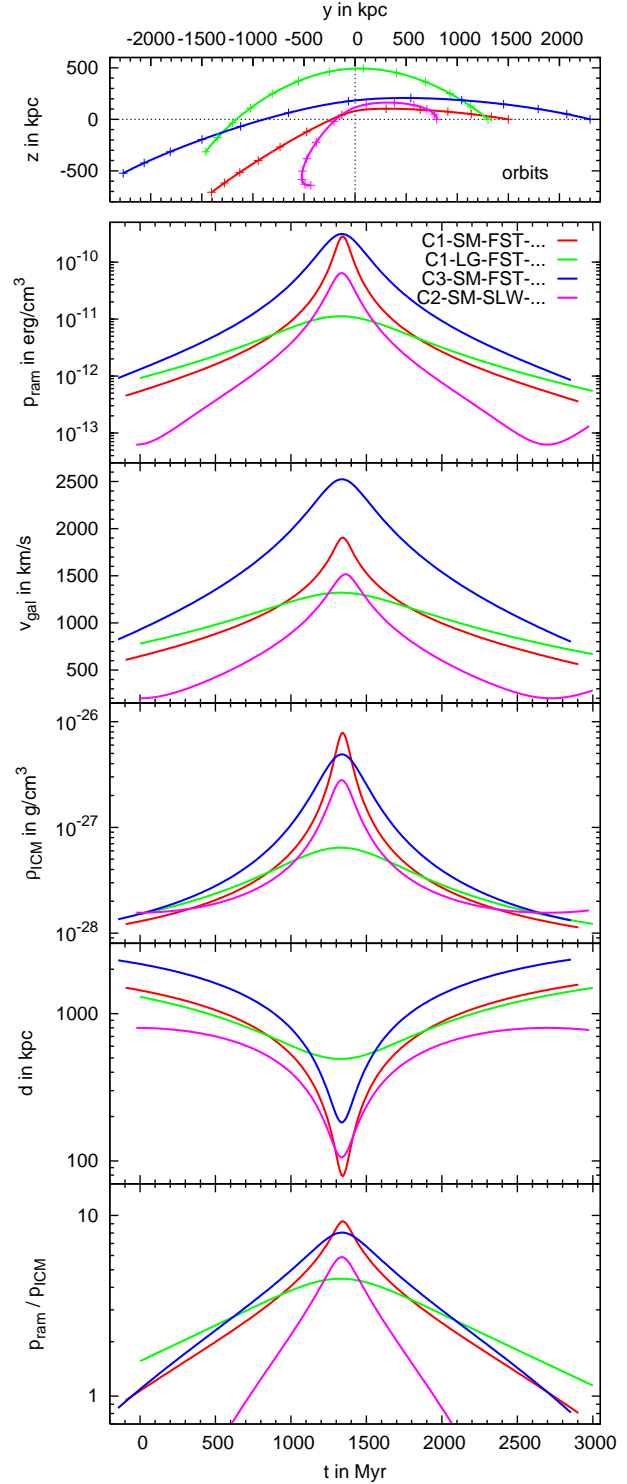


Figure 5. Summary of galaxy orbits for our simulations. The top panel shows the orbits, which are in the y - z -plane. Crosses mark the position of the galaxy in intervals of 250 Myr. The next panels show the temporal evolution of ram pressure, p_{ram} , galaxy velocity, v_{gal} , ICM density along orbit, ρ_{ICM} , distance to cluster centre, d , and ratio between ram pressure and local ICM pressure, $p_{\text{ram}}/\rho_{\text{ICM}}$. For an explanation of the labels see text.

from the galactic potential immediately but with a certain delay, because it takes some time until the gas is accelerated to the escape velocity. This time delay grows with decreasing ram pressure as the ram pressure is responsible for accelerating stripped gas packages.

The second gas removal process is continuous stripping (or turbulent/viscous stripping, see e.g. Nulsen 1982; Quilis et al. 2000), which is caused by the Kelvin-Helmholtz instability induced by the ICM wind flowing over the surface of the gas disc. Continuous stripping leads to a slow but continuous gas loss at a rate of $\sim 1M_{\odot} \text{ yr}^{-1}$, it works on a timescale of Gyrs. The gas disc radius is not changed significantly by continuous stripping.

3.1 Analytical estimates

The usual way to estimate the amount of gas loss due to ram pressure pushing for galaxies moving face-on follows the suggestion of GG72. Here, one compares the gravitational restoring force per unit area,

$$f_{\text{grav}}(R) = \Sigma_{\text{gas}}(R) \frac{\partial \Phi}{\partial Z}(R), \quad (2)$$

and the ram pressure,

$$p_{\text{ram}} = \rho_{\text{ICM}} v_{\text{gal}}^2, \quad (3)$$

for each radius of the galaxy (see e.g. RB06), where Φ is the gravitational potential of the galaxy, $\Sigma_{\text{gas}}(R)$ the gas surface density, ρ_{ICM} the ICM density and v_{gal} the galaxy's velocity. At radii where the restoring force is larger, the gas can be retained, at radii where the ram pressure is larger, the gas will be stripped. The transition radius is called the stripping radius. In order to apply this estimate to our simulations, we compare the gravitational restoring force to the current ram pressure at every time. This estimate should work best for galaxies moving face-on.

(Nearly) pure continuous stripping affects galaxies moving edge-on. All galaxies with other inclinations experience a mixture of ram pressure pushing and continuous stripping. For a spherical gas cloud, the mass loss rate due to continuous stripping was estimated by Nulsen (1982). For a sphere of radius, R , moving through the ICM of density, ρ_{ICM} , with velocity, v_{gal} , the appropriate mass loss rate is $\pi R^2 \rho_{\text{ICM}} v_{\text{gal}}$. As the surface area of a sphere is twice as large as the surface area of a disc (counting upper and lower side), we use

$$\dot{M}_{\text{KH}} = 0.5\pi R^2 \rho_{\text{ICM}} v_{\text{gal}} \quad (4)$$

for our case of a disc galaxy. Both, ICM density, ρ_{ICM} , and galaxy velocity, v_{gal} are time-dependent. As disc radius, R , we use the current analytical stripping radius as estimated by the GG72 criterion, which is also time-dependent. This choice may seem mismatched at first, but it is motivated by the fact that the GG72 criterion gives good results for the stripping radius for most inclinations.

3.2 Snapshots

Figure 6 shows snapshots for run C2-SM-SLW-MFM (high resolution). At larger distances to the cluster centre, the galaxy moves subsonically, in the inner cluster it moves supersonically as indicated by the bow shock. Before pericentre passage, the gas disc size decreases, whereas it stays rather

constant after pericentre passage. Snapshots for other runs are similar.

3.3 Comparison with numerical result

Figure 7 compares analytical estimates and numerical results for the stripping radius and the remaining gas mass. On the way towards the cluster centre, the distinction between the instantaneous and continuous stripping phases vanishes as both processes overlap. In earlier simulations with constant ICM wind (RH05, RB06, but also MBD03) a short period of gas backfall during the intermediate phase was observed. The gas disc mass as a function of time showed a characteristic local maximum after the instantaneous stripping phase. Now, in the simulations with varying ICM wind, we observe a repeated backfall of stripped gas prior and during pericentre passage. The backfall appears as repeated local maxima or plateaus in the gas disc mass as a function of time. Interestingly, the sticky-particle simulations of Vollmer et al. (2001) where the galaxies were also exposed to a varying ram pressure found gas backfall of up to $5 \times 10^8 M_{\odot}$ after pericentre passage, primarily for edge-on galaxies. This behaviour cannot be observed in our simulations. The backfall cycles in our simulations are caused by the hydrodynamical velocity field in the galaxy's wake. On the way out of the cluster, the instantaneous stripping is not active anymore because all gas from outer radii is already lost. Here continuous stripping dominates.

3.3.1 Ram pressure pushing

The result of the analytical estimate that only takes ram pressure pushing into account is shown as black lines in Fig. 7. The analytical and numerical result for the stripping radius agree remarkably well. Only during the pericentre passage in runs C2-SM-SLW-..., the simulated galaxies can retain a larger gas disc than predicted. Here, the ram pressure, p_{ram} , increases faster than the stripping timescale: During the ~ 200 Myr before the ram pressure maximum, the stripping radius is predicted to decrease from 10 kpc to 4 kpc, which corresponds to an average radius decrease of 1 kpc per 35 Myr. A rough estimate of the acceleration of gas with a surface density, Σ , is p_{ram}/Σ . Thus, the stripping timescale, i.e the time needed to move the gas package a distance, s , is

$$\tau = 55 \text{ Myr} \sqrt{\frac{s}{5 \text{ kpc}} \frac{\Sigma}{10^{-3} \text{ g cm}^{-2}} \frac{10^{-11} \text{ erg cm}^{-3}}{p_{\text{ram}}}}, \quad (5)$$

where we have inserted typical values for this case. However, this estimate is a lower limit, as it neglects the effect of the galaxy's restoring force, which lessens the effective acceleration. Although this timescale is rather short, in runs C2-SM-SLW-... the ram pressure changes on an even faster timescale during pericentre passage.

For all other runs, deviations of the gas disc radius from the analytical result can be attributed to different inclinations and they agree with the results of constant ICM wind simulations of RB06. As expected from the simulations of RB06, with an increasing deviation from the face-on inclination, the remaining gas disc becomes increasingly asymmetrical. This behaviour translates into an increasing distance

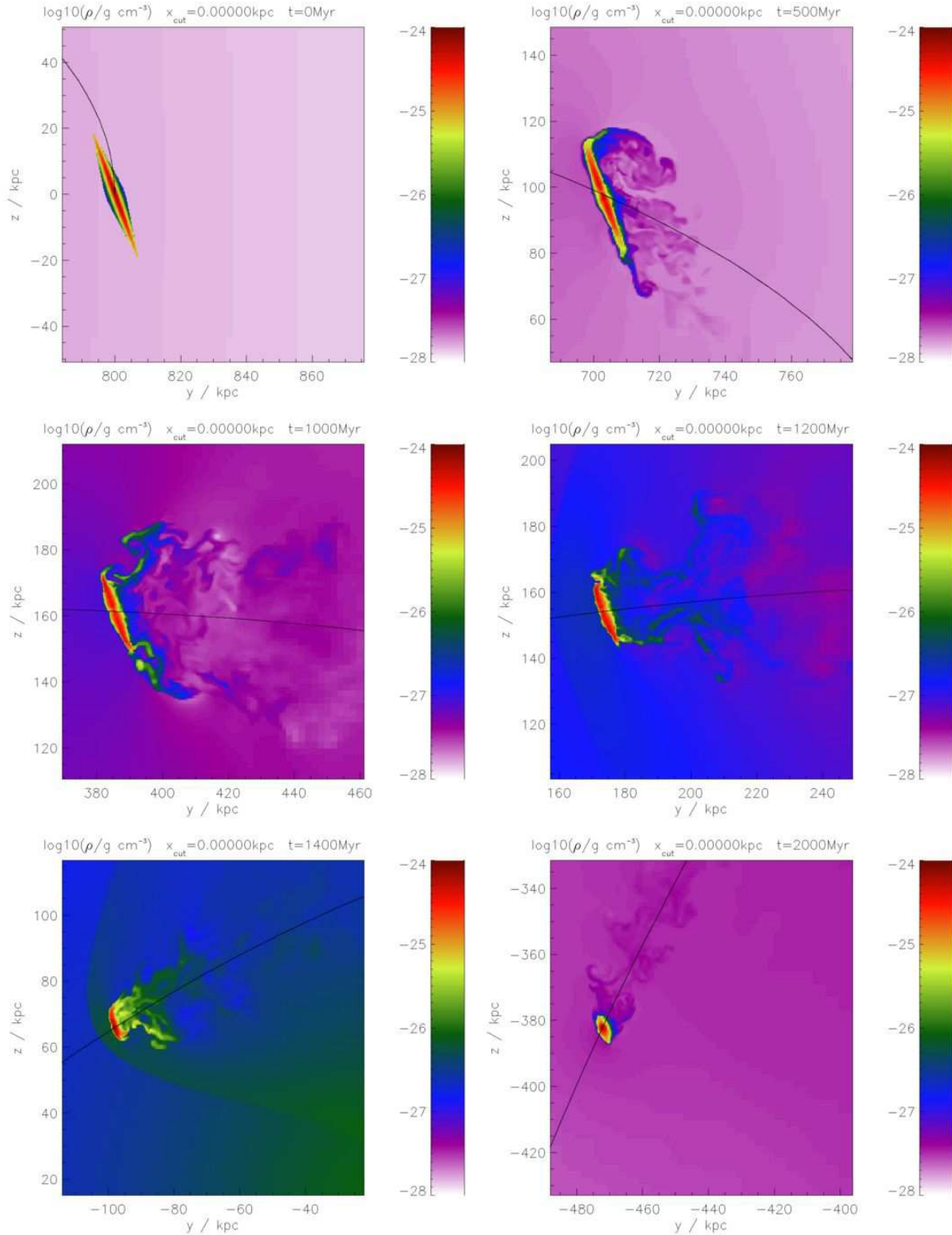


Figure 6. Snapshots for run C2-SM-SLW-MFM (high resolution): colour-coded gas density in the orbital plane. The black line marks the galaxy orbit.

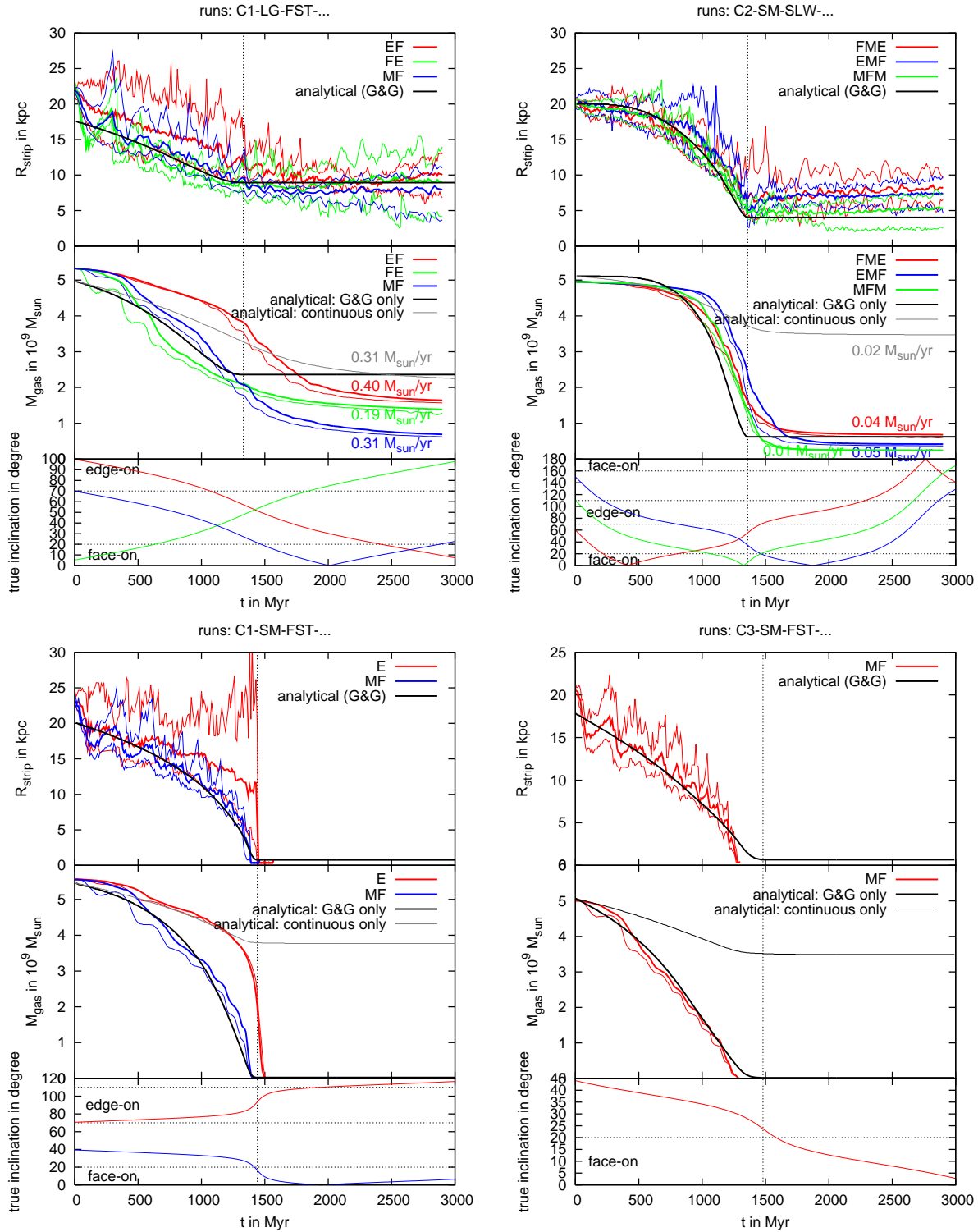


Figure 7. Comparison between analytical and numerical stripping radius (top panels) and gas mass (middle panels). The bottom panels display the evolution of the true inclination, i.e. the angle between the galaxy’s rotation axis and the direction of motion. Each subfigure is for one orbit (see title), different inclinations are colour-coded (see legend). For the numerical stripping radius, the mean value (thick lines) as well as maximum and minimum radius (thin lines) as described in RB06 are shown. For the gas mass, we show the bound gas mass (thick lines) and the mass of gas in the disc region (thin lines of matching colour, see also RB06). Analytical estimates according to the Gunn&Gott criterion are shown as black lines for the stripping radius as well as for the remaining gas mass. The gray line in the mass plots displays the predicted remaining gas mass if only continuous stripping is taken into account. In cases where the galaxy was not stripped completely, we did a linear fit for the bound gas mass for the final Gyr of the simulations as well as for the analytical estimate of continuous stripping. The resulting mass loss rates are denoted colour-coded in the plot.

between the minimum and maximum radius lines in Fig. 7. A further agreement with the constant wind simulations is the fact that for the highest ram pressure peak, the galaxy is stripped completely even if it is moving near-edge-on (run C1-SM-FST-E).

The slightly premature complete stripping of the galaxies in runs C1-SM-FST-MF and C3-SM-FST-MF is caused by the fact that the remaining gas disc is affected by numerical diffusion due to the relatively low resolution of 0.5 kpc. Details are discussed in App. A. All other results concerning ram pressure pushing are not affected by numerical diffusion or resolution.

For the remaining gas mass, the simple analytical estimate and the numerical results agree only roughly. Generally, in the simulations the galaxies lose their gas more slowly than predicted, because the analytical estimate does not include the delay in mass loss explained above (Sect. 3.1). Moreover, it neglects effects of inclination and continuous stripping.

3.3.2 Continuous stripping

The gray line in the mass plots in Fig. 7 displays the analytical estimate for the remaining gas mass if purely continuous stripping (see Eq. 4) is taken into account. Before pericentre passage, this is most likely to apply to galaxies moving edge-on. Indeed, we find a good agreement in mass loss rate for the first Gyr of runs C1-LG-FST-EF and C1-SM-FST-E, where this condition is fulfilled. For C2-SM-SLW-EMF, the ram pressure is very small during the first Gyr and thus the delay in mass loss is long. Therefore, the mass loss rate is overpredicted here.

Pure continuous stripping is also expected to apply to the time well after pericentre passage. Thus, we have calculated averaged mass loss rates for the final Gyr of the simulations. We have also calculated the averaged mass loss rate for this time interval from the analytical prediction by Eq. 4. The values are given in Fig. 7. The mass loss rates at this late stage of the simulations have to be interpreted as upper limits, because due to the relatively low resolution of 0.5 kpc the remaining gas disc is already significantly affected by numerical diffusion (see Sect. A for a detailed discussion).

4 DISCUSSION AND SUMMARY

We have presented 3D hydrodynamical simulations of RPS of a disc galaxy orbiting in a galaxy cluster. We have focused on the evolution of the radius of the remaining gas disc and the mass of gas bound to the galaxy. In particular, we compared the numerical results to a time-dependent version of the classical GG72 estimate.

For galaxies not moving near edge-on, we find that the stripping radius is predicted well by the estimate based on the GG72 criterion, unless the ram pressure increases faster than the stripping timescale. Then the remaining gas disc is somewhat larger than predicted. However, the evolution of the bound gas mass differs between simulations and the analytical estimate: In the simulations, the galaxy loses the gas more slowly than predicted. Deviations of the analytical estimate from the simulation results are caused by effects that

are not taken into account by the estimate: the inclination of the galaxy, the time delay of true gas loss, and the combined effect of ram pressure pushing and continuous stripping. Although our simulations are an important step towards realistic models of RPS, they also neglect some aspects that have to be studied in the future, e.g. the multiphase physics of the ISM and transport processes and ambient motions in the ICM.

The differences between analytical estimate and simulations in the evolution of the remaining gas mass will also be reflected in the distribution of stripped ISM throughout the cluster. If galaxies followed the prediction of the estimate based on the GG72 criterion, they would not lose gas after pericentre passage. In the simulations, however, they do. Thus, the distribution of the stripped ISM along the orbit is broader than expected.

ACKNOWLEDGEMENTS

We acknowledge the support by the DFG grant BR 2026/3 and the supercomputing grants NIC 2195 and 2256 at the John-Neumann Institut (NIC) in Jülich. The results presented were produced using the FLASH code, a product of the DOE ASC/Alliances-funded Center for Astrophysical Thermonuclear Flashes at the University of Chicago.

APPENDIX A: INFLUENCE OF RESOLUTION

In order to check the influence of the resolution on our results, we repeated two runs with better resolution. Run C1-LG-FST-MF was repeated such that the resolution was improved by a factor of 2 everywhere in the grid compared to the description in Sect. 2.1. Run C2-SM-SLW-MFM was repeated such that the inner disc region, i.e. a cylinder around the galactic centre with radius 10 kpc and thickness 6 kpc, was always refined to 0.25 kpc.

In grid-codes, advection of mass and momentum into non-axial directions is always accompanied by a numerical viscosity due to numerical diffusion. In the rotating gas disc, the gas has to move on circular orbits in a Cartesian grid. This geometrical mismatch is strongest in the inner part of the galaxy. Below a certain radius, the resolution of the rotational motion becomes insufficient and the numerical diffusion introduces radial velocities, which lead to a decrease of the central density. Fig. A1 shows an example for this effect. As expected, the decrease in central density is much weaker if higher resolution is used. Interestingly, it is also less pronounced for galaxies moving near edge-on.

For the evolution of the galaxy's gas disc mass and radius, two consequences arise from this effect:

Firstly, in cases where the galaxy moves with medium to face-on inclination, not only the central density, but also the central projected surface density, Σ , decreases, though much milder. The decrease in surface density makes the gas disc more vulnerable to ram pressure pushing (compare to Eq. 2). For quite strong ram pressures as in run C2-SM-SLW-MFM, this could cause the galaxy centre to be stripped prematurely. This indeed happened in the low resolution case of run C2-SM-SLW-MFM. In the high resolution case,

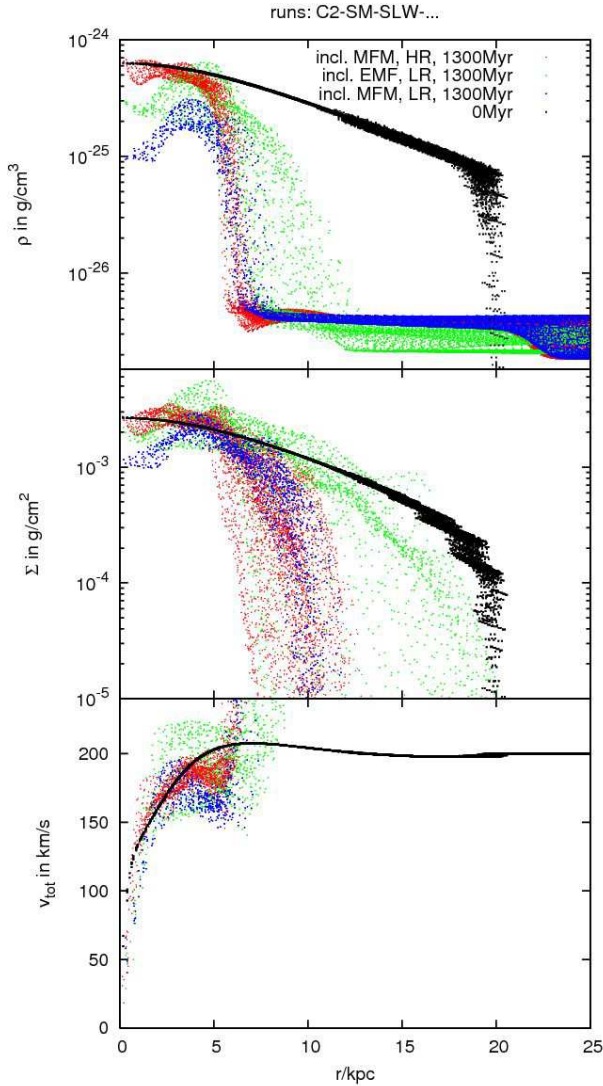


Figure A1. Radial profiles of the density, ρ , projected surface density, Σ , and total velocity, v_{tot} , in the galactic plane at $t = 1300$ Myr for different runs along the orbit C2-SM-SLW (see legend). One dot for each cell in the galactic plane is plotted. Black dots show the initial profile. Red and blue dots are for runs with inclination MFM, but different resolution (red for $\Delta x = 0.25$ kpc, denoted “HR” in the legend; blue for $\Delta x = 0.5$ kpc, denoted “LR”). Green dots are for inclination EMF and also resolution $\Delta x = 0.5$ kpc.

the gas loss behaves as expected. Fig. A2 shows the evolution of mass and radius for the two different resolutions. Up to pericentre passage, the two runs are nearly identical. The only other “critical” cases in the sense described above are the runs C1-SM-FST-MF and C3-SM-FST-MF. For both runs, the gas disc radius and mass evolution agrees well with the analytical estimate up to shortly before pericentre passage. In both runs, the galaxy is stripped completely shortly before pericentre passage, which is slightly faster than predicted by the analytical estimate. We conclude that this sudden gas loss shortly before pericentre passage is due to the numerical effect described above. However, we also conclude that the galaxies would indeed be stripped completely as the

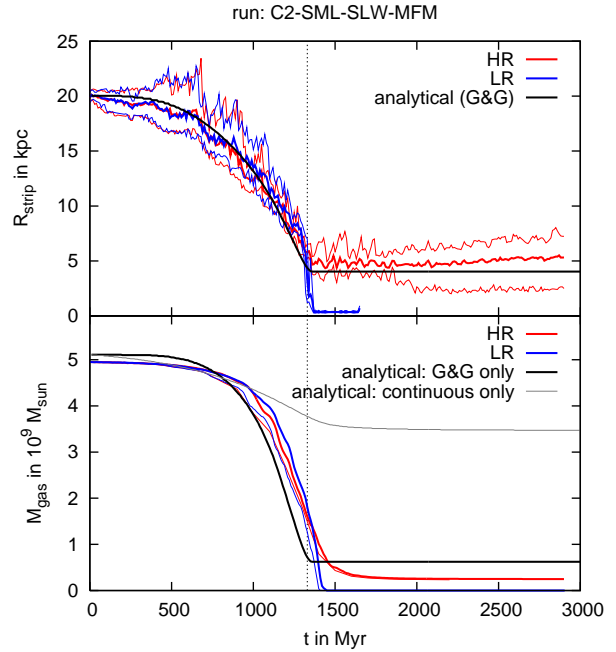


Figure A2. Same as Fig. 7, but comparing the high resolution (HR) and low resolution (LR) run for case C2-SM-SLW-MFM.

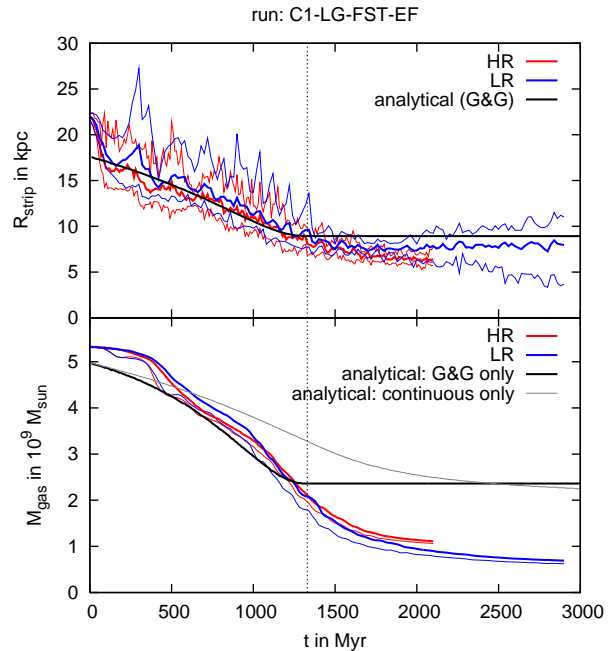


Figure A3. Same as Fig. A2, but comparing the high resolution (HR) and low resolution (LR) run for case C1-LG-FST-EF.

one in run C1-SM-FST-E is stripped completely but is not expected to suffer strongly from the numerical viscosity, as shown in Fig. A1.

The second consequence concerns continuous stripping. Figure A3 compares the evolution of the mass and radius for run C1-LG-FST-EF for two different resolutions. Up to ~ 1500 Myr, both results agree very well. After that, the low resolution run yields a higher mass loss rate than the high

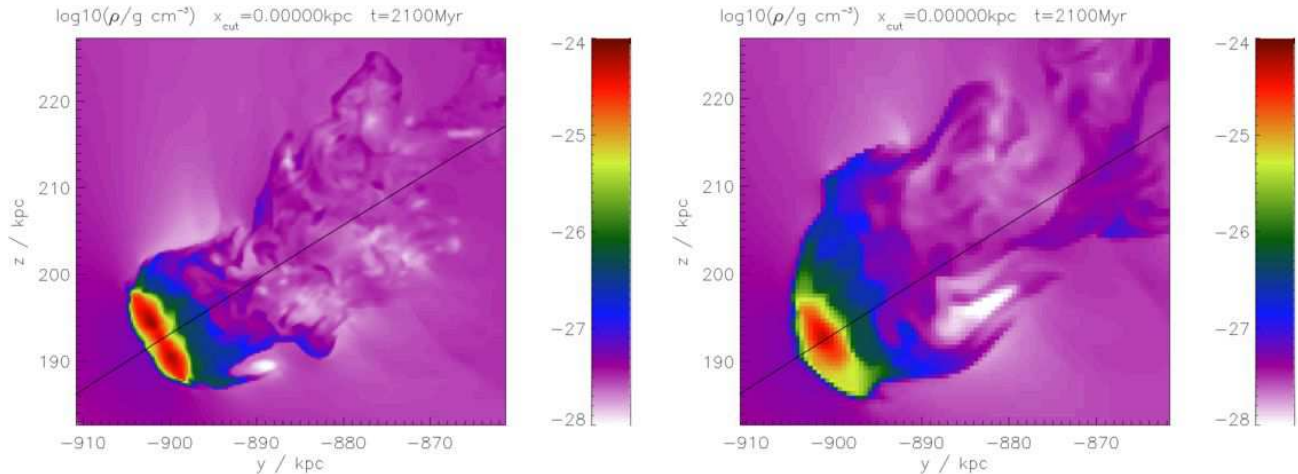


Figure A4. Colour-coded gas density in the orbital plane for run C1-LG-FST-EF, at time $t = 2100$ Myr. The left panel is for high resolution (HR), the right panel for low resolution (LR). The black line marks the galaxy's orbit.

resolution run. This is due to the fact that the influence of the numerical diffusion on the shape of the remaining gas disc is no longer negligible, as can be seen in Fig. A4.

Concerning the evolution of the mass and radius of the remaining gas disc, we conclude that the results presented in Fig. 7 are reliable at least up to pericentre passage. After pericentre passage, the mass loss rates due to continuous stripping derived by our simulations, are upper limits.

REFERENCES

- Abadi M. G., Moore B., Bower R. G., 1999, *MNRAS*, 308, 947
- Acreman D. M., Stevens I. R., Ponman T. J., Sakelliou I., 2003, *MNRAS*, 341, 1333
- Fryxell B., Olson K., Ricker R., Timmes F. X., Zingale M., Lamb D. Q., MacNeice P., Rosner R., Truran J. W., Tufo H., 2000, *ApJS*, 131, 273
- Goto T., Yamauchi C., Fujita Y., Okamura S., Sekiguchi M., Smail I., Bernardi M., Gomez P. L., 2003, *MNRAS*, 346, 601
- Gunn J. E., Gott J. R., 1972, *ApJ*, 176, 1
- Lea S. M., Young D. S. D., 1976, *ApJ*, 210, 647
- Marcolini A., Brighenti F., A.D'Ercole 2003, *MNRAS*, 345, 1329
- Matsumoto H., Tsuru T. G., Fukazawa Y., Hattori M., Davis D. S., 2000, *PASJ*, 52, 153
- Mohr J. J., Mathiesen B., Evrard A. E., 1999, *ApJ*, 517, 627
- Moore B., Katz N., Lake G., Dressler A., Oemler A., 1996, *Nature*, 379, 613
- Moore B., Lake G., Katz N., 1998, *ApJ*, 495, 139
- Moore B., Lake G., Quinn T., Stadel J., 1999, *MNRAS*, 304, 465
- Nulsen P. E. J., 1982, *MNRAS*, 198, 1007
- Quilis V., Moore B., Bower R., 2000, *Science*, 288, 1617
- Roediger E., Brüggem M., 2006, *MNRAS*, 369, 567
- Roediger E., Hensler G., 2005, *A&A*, 433, 875
- Schulz S., Struck C., 2001, *MNRAS*, 328, 185

Takeda H., Nulsen P. E. J., Fabian A. C., 1984, *MNRAS*, 208, 261

Toniazzo T., Schindler S., 2001, *MNRAS*, 325, 509

van Gorkom J. H., 2004, in Mulchaey J. S., Dressler A., Oemler A., eds, *Clusters of Galaxies: Probes of Cosmological Structure and Galaxy Evolution Vol. 3 of Carnegie Observatories Astrophysics Series, Interaction of galaxies with the intracluster medium*. Cambridge University Press, Cambridge, p. 306

Vollmer B., 2003, *A&A*, 398, 525

Vollmer B., Braine J., Balkowski C., Cayatte V., Duschl W. J., 2001, *A&A*, 374, 824

Vollmer B., Cayatte V., Balkowski C., Duschl W. J., 2001, *ApJ*, 561, 708

Vollmer B., Cayatte V., Boselli A., Balkowski C., Duschl W. J., 1999, *A&A*, 349, 411

Vollmer B., Marcelin M., Amram P., Balkowski C., Cayatte V., Garrido O., 2000, *A&A*, 364, 532

This paper has been typeset from a \TeX / \LaTeX file prepared by the author.